Supplemental Materials

Molecular Biology of the Cell

Escorcia and Forsburg

Recombination dynamics and relative spore viability of dmc1Δ cells					
	Chr	**Genetic Distance cM**		**Fold Reduction**	**p-value[b]**
Intergenic interval		**WT**	**dmc1Δ**	**dmc1Δ**	**dmc1Δ**
his4-lys4[a]	2	6.81 ± 0.92	4.70 ± 0.82	1.45	p<0.01
Intragenic interval[d]	**Chr**	**Frequency (x10^3)**		**Fold Reduction**	**p-value[c]**
ade6-M26-52	3	3.34 ± 0.08 (60/17987)	1.90 ± 1.20 (9/4696)	1.76	0.2184
		% relative viability		**% Reduction**	**p-value[c]**
		100.00 ± 0.47	85.87 ± 1.57	14.13	p<0.05

[a]Markers in this interval were scored in repulsion (+-/-+).

[b]Significance calculated by 2-tail student *t*-test.

[c]Significance calculated by chi-squared analysis.

[d]Frequency values were calculated by dividing number of ade+ by total number of colonies screened (shown in parenthesis).

List of strains used in this work			
FY number	**Genotype**	**Figure or Table**	**Source**
7	h-	1A; S1A	lab stock
8	h+	1A; S1A	lab stock
9	h- leu1-32	Table 1	lab stock
527	h- his3-D1 ade6-M216 ura4-D18 leu1-32	1A; S1A	lab stock
528	h+ his3-D1 ade6-M210 ura4-D18 leu1-32	1A; S1A	lab stock
1251	h+ ade6-M26 his4-239	Table 1	lab stock
1668	h- dmc1Δ::ura4+ ade6-52 lys4-95 ura4-D18	STable 1	lab stock
1669	h+ dmc1Δ::ura4+ ade6-M26 his4-239 ura4-D18	STable 1	lab stock
2057	h- pat1-114 ade6-M216 can1-1	1B-D; S2A	lab stock
3226	h- Δswi1::kanmx ura4-D18 leu1-32 ade6-M210 his3-D1	1A; S1A	lab stock
3227	h+ Δswi1::KanMX ura4-D18 leu1-32 ade6-M210 his3-D1	1A; S1A	lab stock
3228	h+ Δswi3::KanMX ura4-D18 leu1-32 ade6-M210 his3-D1	1A; S1A	lab stock
3229	h- Δswi3::KanMX ura4-D18 leu1-32 ade6-M210	1A; S1A	lab stock
3500	h90 mat2-102 pat1-114 ade6-M210	1B-D; S2A	lab stock
3985	h- Δrec12::ura4+ ura4-D18 leu1-32 ade6-M210	1A; S1A	lab stock
3986	h- Δrec12::ura4+ ura4-D18 ade6-M210	1A; S1A	lab stock
4588	h+ Δswi1::kanMX	S1A	lab stock
5207	h- lys4-95 ade6-52	Table 1	lab stock
5608	h- hht1-mRFP:KanMX6 leu1-32 ura4-D18	3A-D	lab stock
5609	h+ hht1-mRFP:KanMX6 leu1-32 ura4-D18	3A-D	lab stock
5786	h- hht1-mRFP:kanMX his7+::lacI-GFP lys1+::lacO leu1-32 ura4-D18	4A-D; 5A-D	lab stock
5787	h+ hht1-mRFP:kanMX his7+::lacI-GFP lys1+::lacO leu1-32 ura4-D18	4A-D; 5A-D	lab stock
6699	h- pat1-114 Δswi3::KanMX6 ade6-M210	1B-D; S2A	this study
6858	h90 mat2-102 pat1-114 Δswi3::KanMX6 ade6-M216	1B-D; S2A	this study
6859	h- pat1-114 Dswi1::KanMX6 ade6-M216	1B-D; S2A	this study
6983	h- Δswi1::KanMX6 ade6-M26 his4-239	Table 1	this study
7041	h+ Δswi1::KanMX6 ade6-52 lys4-95	Table 1	this study
7042	h- Δswi3::KanMX6	S1A	this study
7229	h+ Δswi3::KanMX6 ade6-M26 his4-239	Table 1	this study

7234	h90 mat2-102 pat1-114 Δswi1::KanMX6 ade6-M210	1B-D; S2A	this study
7299	h- Δswi3::KanMX6 ade6-52 lys4-95	Table 1	this study
7300	h+ Δswi1::KanMX6 ura4-D18 leu1-32 ade6-m210 hht1-mRFP:KanMX6 his7+lacI-GFP lys1+:lacO	4A-D; 5A-D	this study
7301	h- Δswi1::KanMX6 ura4-D18 leu1-32 ade6-m210 hht1-mRFP:KanMX6	4A-D; 5A-D	this study
7302	h- Δswi3::KanMX6 ura4-D18 leu1-32 ade6-m210 his3-D1 hht1-mRFP:KanMX6	3A-D; 4A-D; S3A-C	this study
7303	h+ Δswi3::KanMX6 ura4-D18 leu1-32 ade6-m210 hht1-mRFP:KanMX6 lys1+:lacO	4A-D; 5A-D	this study
7310	h- Δswi3::KanMX6 ura4-D18 leu1-32 ade6-m210 hht1-mRFP:KanMX6 his7+lacI-GFP lys1+:lacO	4A-D; 5A-D	this study
7320	h+ Δswi1::KanMX6 ura4-D18 leu1-32 ade6-m210 his3-D1 hht1-mRFP:KanMX6	3A-D; 4A-D; S3A-C	this study
7415	h- Δswi1::KanMX6 ura4-D18 leu1-32 ade6-m210 rec8-GFP:Kan(YW) hht1-mRFP:KanMX6	8A-E; S4A-G	this study
7416	h- Δswi3::KanMX6 ura4-D18 leu1-32 ade6-m210 his3-D1 rec8-GFP:Kan(YW) hht1-mRFP:KanMX6	8A-E; S4A-G	this study
7444	h+ Δswi1::KanMX6 ura4-D18 leu1-32 ade6-m210 rec8-GFP:Kan(YW) hht1-mRFP:KanMX6	8A-E; S4A-G	this study
7445	h+ Δswi3::KanMX6 ura4-D18 leu1-32 ade6-m210 rec8-GFP:Kan(YW) hht1-mRFP:KanMX6	8A-E; S4A-G	this study
7450	h- Δswi1::KanMX6 Δrec12::ura4+ ura4-D18 leu1-32 ade6-m210	1A; S1A	this study
7451	h+ Δswi1::KanMX6 Δrec12::ura4+ ura4-D18 leu1-32 ade6-m210 his3-D1	1A; S1A	this study
7454	h- Δswi3::KanMX6 Δrec12::ura4+ ura4-D18 leu1-32 ade6-m210 his3-D1	1A; S1A	this study
7455	h+ Δswi3::KanMX6 Δrec12::ura4+ ura4-D18 leu1-32 ade6-m210 his3-D1	1A; S1A	this study
7469	h+ hht1-mRFP:KanMX6 rad11-Cerulean::hphMX rad22-YFP-natMX leu1-32 ade6-M210 ura4-D18 (rad11=ssb1)	2A-D	lab stock
7470	h- hht1-mRFP:KanMX6 rad11-Cerulean::hphMX rad22-YFP-natMX leu1-32 ade6-M210 ura4-D18 (rad11=ssb1)	2A-D	lab stock
7538	h90 mat2-102 pat1-114 Δswi3::KanMX6 Δrec12::ura4+ ura4-D18 ade6-m210	S1B-D; S2B	this study
7540	h- pat1-114 Δswi3::KanMX6 Δrec12::ura4+ ura4-D18 ade6-m216	S1B-D; S2B	this study
7544	h90 mat2-102 pat1-114 Δswi1::KanMX6 Δrec12::ura4+ ura4-D18 ade6-m210	S1B-D; S2B	this study
7547	h- pat1-114 Δswi1::KanMX6 Δrec12::ura4+ ura4-D18 ade6-m216	S1B-D; S2B	this study
7561	h+ Δswi1::KanMX Δswi3::KanMX6 ura4-D18 leu1-32 ade6-M210 his3-D1	1A	this study
7562	h- Δswi1::KanMX Δswi3::KanMX6 ura4-D18 leu1-32 ade6-M210 his3-D1	1A	this study
7564	h- pat1-114 Δswi3::KanMX6 ura4-D18 ade6-M210 rec8-GFP:Kan(YW)	S4E	this study
7572	h90 mat2-102 pat1-114 Δswi3::KanMX6 ade6-216 rec8-GFP:Kan(YW) hht1-mRFP:KanMX6	S4E	this study
7574	h90 mat2-102 pat1-114 Δswi1::KanMX6 ade6-210 rec8-GFP:Kan(YW)	S4E	this study
7576	h- pat1-114 Δswi1::KanMX6 ade6-216 rec8-GFP:Kan(YW)	S4E	this study
7593	h- Δswi1::KanMX6 ura4-D18 leu1-32 ade6-m210 hht1-mRFP:KanMX6 rad11-Cerulean:hphMX rad22-YFP:natMX	2A-D	this study
7594	h+ Δswi1::KanMX6 ura4-D18 leu1-32 ade6-m210 hht1-mRFP:KanMX6 rad11-Cerulean:hphMX rad22-YFP:natMX	2A-D	this study
7598	h- Δswi3::KanMX6 ura4-D18 leu1-32 ade6-m210 hht1-mRFP:KanMX6 rad11-Cerulean:hphMX rad22-YFP:natMX	2A-D	this study
7602	h+ Δswi3::KanMX6 ura4-D18 leu1-32 ade6-m210 hht1-mRFP:KanMX6 rad11-Cerulean:hphMX rad22-YFP:natMX	2A-D	this study

7663	h+ leu2-120	Table 1	this study
7664	h- ura2-10	Table 1	this study
7666	h+ his7-36	Table 1	this study
7670	h- Δswi1::KanMX6 leu2-120	Table 1	this study
7672	h+ Δswi1::KanMX6 ura2-10	Table 1	this study
7674	h+ Δswi1::KanMX6 leu1-32	Table 1	this study
7675	h- Δswi1::KanMX6 his7-36	Table 1	this study
7677	h+ Δswi3::KanMX6 leu2-120	Table 1	this study
7678	h- Δswi3::KanMX6 ura2-10	Table 1	this study
7679	h- Δswi3::KanMX6 leu1-32	Table 1	this study
7681	h+ Δswi3::KanMX6 his7-36	Table 1	this study
7748	h- rec8-GFP:KanMX6 hht1-mRFP:KanMX6 pat1-114 ura4-D18 ade6-m216	8A-E; S4E-G	this study
7777	h+ rec27-205-GFP-KanMX hht1-mRFP:KanMX6 pat1-114 ura4-D18 ade6-3049 lys4-95	6A-E; S4A-B	this study
7779	h- rec27-205-GFP-KanMX hht1-mRFP:KanMX6 pat1-114 ura4-D18 ade6-3049 lys4-95	6A-E; S4A-B	this study
7780	h+ Δswi1::KanMX6 rec27-205-GFP-KanMX hht1-mRFP:KanMX6 pat1-114 leu1-32 ade6- his- lys4-95	6A-E; S4A-B	this study
7781	h- Δswi1::KanMX6 rec27-205-GFP-KanMX hht1-mRFP:KanMX6 pat1-114 ade6-	6A-E; S4A-B	this study
7783	h- Δswi3::KanMX6 rec27-205-GFP-KanMX hht1-mRFP:KanMX6 pat1-114 ade6-	6A-E; S4A-B	this study
7784	h+ Δswi3::KanMX6 rec27-205-GFP-KanMX hht1-mRFP:KanMX6 pat1-114 leu1-32 ade6-	6A-E; S4A-B	this study
7840	h+ rec8-GFP:KanMX6 hht1-mRFP:KanMX6 pat1-114 ura4-D18 ade6-m210	8A-E; S4E-G	this study
7863	h+ sgo1-FLAG:GFP hht1-mRFP:KanMX6 ura4-D18 leu- ade6-M210 his3-D1	7A-E; S4C-D	this study
7864	h- sgo1-FLAG:GFP hht1-mRFP:KanMX6 ura4-D18 leu- ade6-M210	7A-E; S4C-D	this study
7902	h90 mat2-102 pat1-114 Δrec12::ura4+ ura4-D18 ade6-M210	S1B-D; S2B	this study
7907	h- pat1-114 Δrec12::ura4+ ura4-D18 leu1-32 ade6-M216	S1B-D; S2B	this study
8121	h- Δswi1::KanMX6 ura4-D18 leu1-32 hht1-mRFP:KanMX6 his7+lacI-GFP lys1+:lacO	4A-D; 5A-D	this study
8122	h+ Δswi3::KanMX6 ura4-D18 leu1-32 ade6-m210 his3-D1 hht1-mRFP:KanMX6 his7+lacI-GFP lys1+:lacO	4A-D; 5A-D	this study
8123	h- cnp1-mCherry:KanMX6 swi6-GFP:KanMX6 ura4-D18 leu1-32 ade6-M210	9A-D	this study
8125	h- Δswi1::KanMX6 cnp1-mCherry:KanMX6 swi6-GFP:KanMX6 ura4-D18 leu1-32 ade6-M210	9A-D	this study
8126	h+ Δswi1::KanMX6 cnp1-mCherry:KanMX6 swi6-GFP:KanMX6 ura4-D18 leu1-32 ade6-M210	9A-D	this study
8127	h+ Δswi3::KanMX6 cnp1-mCherry:KanMX6 swi6-GFP:KanMX6 ura4-D18 leu1-32 ade6-M210	9A-D	this study
8128	h- Δswi3::KanMX6 cnp1-mCherry:KanMX6 swi6-GFP:KanMX6 ura4-D18 leu1-32 ade6-M210	9A-D	this study
8129	h90 mat2-102 pat1-114 rec8-GFP:KanMX6 hht1-mRFP:KanMX6 leu1-32 ade6-M210	S4E	this study

8172	h+ cnp1-mCherry:KanMX6 swi6-GFP:KanMX6 ura4-D18 leu1-32 ade6-M210	9A-D	this study
8180	h+ Δswi1::KanMX6 sgo1-GFP:KanMX6 hht1-mRFP:KanMX6 ura4-D18 leu1-32 ade6-M210 his3-D1	7A-E; S4C-D	this study
8181	h+ Δswi3::KanMX6 sgo1-GFP:KanMX6 hht1-mRFP:KanMX6 ura4-D18 leu1-32 ade6-M210 his3-D1	7A-E; S4C-D	this study
8182	h- Δswi3::KanMX6 sgo1-GFP:KanMX6 hht1-mRFP:KanMX6 ura4-D18 leu1-32 ade6-M210 his3-D1	7A-E; S4C-D	this study
8195	h- Δswi1::KanMX6 sgo1-GFP:KanMX6 hht1-mRFP:KanMX6 ura4-D18 leu1-32 ade6-M210	7A-E; S4C-D	this study

SUPPLEMENTAL FIGURE LEGENDS

Supplemental Figure 1. Characterization of fork destabilization in the absence of Rec12. (**A**) Plating efficiency was carried out to determine if lack of the FPC components affects cell viability similarly to spore viability. Logarithmic mitotic cells were counted and plated on YES agar. Resulting colony number per plate was divided by the initial microscope cell count. Percent figures indicate viability for each genotype and are presented relative to those of the wild type strain. n≥4000 cells per genotype. Significance was calculated using chi-squared analysis. Error bars represent 95% confidence intervals. *p*-values are reported as follows: ***p<0.001. Synchronous meiosis in mat2-102/h- pat1-114/pat1-114 diploids was performed for 8 hours. For (**B-D**), hour 0 denotes the time when cells were switched from 25^{o}C to 34^{o}C to elicit meiotic induction. Cells were harvested every hour and examined as indicated in each panel. (**B**) FACS profiles showing progression of replication through meiotic induction. DNA doubling is denoted as the change from 2C to 4C DNA content. Images are representative of three independent trials. (**B**) Pulsed field gel electrophoresis used to separate whole chromosomes by size and to assess formation and repair of meiotic DSBs. Smears migrating faster than chromosome III represent DSBs. Images of ethidium bromide-stained agarose gels represent three different trials. (**C**) DAPI-stained nuclei were counted for each time point to ascertain progression through meiotic divisions, which are reported as follows: black stands for 1 nucleus, dark-gray for 2 nuclei, and light-gray for 3 or more nuclei (3+). 2 and 3+ nuclei indicate onset of MI and MII, respectively. Significance was calculated using chi-squared analysis.

Supplemental Figure 2. Quantification of PGFE. (**A**) Graph showing the signal ratio values of DSB formation and repair in wild type cells and the FPC mutants. (**B**) Graph showing the signal ratio values of DSB formation and repair in cells lacking Rec12 as well as Rec12 and the FPC mutants. Time points correspond to those shown in **Figure 1B-D** and **Supplemental Figure 1B-D**. Hour 0 denotes the time when cells were switched from 25^{o}C to 34^{o}C to elicit meiotic induction. To determine significance, a one-way ANOVA test followed by Tukey family-wise comparison was used. *p*-values were greater than 0.05 in both panels. For visual clarity, error bars represent SEM. Figure panels summarize the average of 3 independent experiments.

Supplemental Figure 3. Lagging chromosomes during MI & MII upon fork destabilization. (**A**) Live-cell images of meiotic cells carrying fluorescently tagged Hht1. Panels are divided into individual fluorescent channels. Bright field panels are omitted due to space limitations. A false-color image was generated to show merged channels. Dotted cell outlines are overlaid on panels for easier visualization of meiotic cells. Minute 0 (0') denotes the last nuclear mass contraction in metaphase I before homologous chromosomes separate in anaphase I (10'). Images that show the characteristics of each reported mutant phenotype were used. Displayed time frames were chosen for optimal representation of nuclear dynamics. (**B**) & (**C**) Quantification of lagging chromosomes in MI & MII from microscopy images shown in (**A**). More than 150 cells were scored from at least two independent movies for each genotype. Chi-squared analysis was used to determine significance. *p*-values are reported as follows: p<0.001 ***. Error bars represent 95% confidence intervals.

Supplemental Figure 4. Timing of Rec27-GFP, Sgo1-GFP, and Rec8-GFP in relation to the meiotic divisions. (**A & D**) Schematic diagrams showing the timing of linear elements elimination and shugoshin duration at the centromere during metaphase. (**G**) Schematic diagram showing the duration of Rec8-GFP foci between MI & MII. (**B**, **C**, **& F**) Time quantification of asci without the specified signal before MI. (**E**) Box plot of Rec8-GFP localization at the centromere at three distinct stages: late metaphase, early MI, and early MII. Each box contains values for 3 independent chromatin immunoprecipitation experiments (with at least two technical replicates per trial) followed by Q-PCR. Tukey whiskers are used to show data points that are less than 1.5 x inter-quartile range (IQR) from the first and third quartiles. Fold values were calculated using the $2^{-\Delta\Delta Ct}$ (Livak) Method (Livak and Shmittgen, 2001). To determine fold change in cohesion, the input and the immuno-precipitated (IP) fractions were used as the calibrator and test parameters, respectively, while *act1* was used as the reference gene (testing for Rec8-GFP localization at the euchromatin) and the centromeric *dg* locus as the target locus (testing for Rec8-GFP localization at the heterochromatin-rich centromere). Significance was determined using a Wilcoxon signed-ranked test. Panels **A**, **D**, and **G** show diagrams of the timing information presented in **Figure 6E**, **Figure 7E**, and **Figure 8E** in the context of metaphase I and the two meiotic divisions. Black arrows with white stripes indicate time progression toward MI, except for Rec8-GFP, which is shown between MI and MII. The distance between each white stripe

denotes 10 minutes. A 10-minute bar is provided for visual reference at the bottom of each diagram. Dotted lines extending toward MI show the time between signal termination and start of meiotic segregation. For all movies, more than 150 cells were scored from at least two independent movies for each genotype. A one-way ANOVA test followed by Tukey family-wise comparison was used to calculate significance. *p*-values are reported as follows: $p<0.01$ **, $p<0.001$ ***. Error bars represent 95% confidence interval.

Supplemental Figure 5. Statistical summary of experiments in this study. Heat map showing *p*-values for each experimental question addressed in this work. Column labels show pair-wise comparisons between the WT and the FPC mutants and between each FPC component. Row labels indicate each studied experimental question. The *p*-value index provides a color gradient representing *p*-value ranges obtained in each experiment. The darker the color, the more significant the result and vice versa.

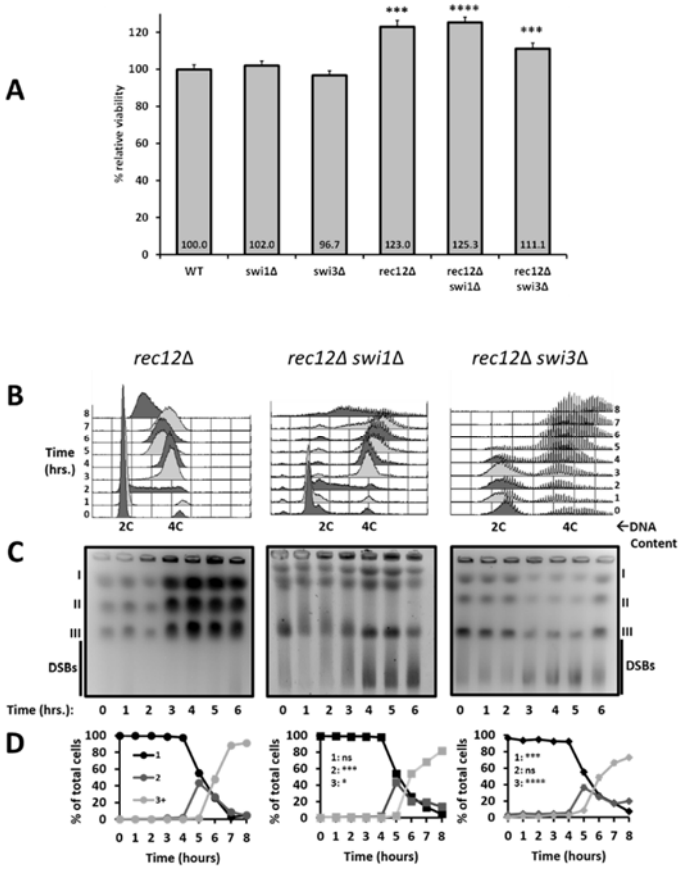
A
% relative viability
100.0
102.0
96.7
123.0
125.3
111.1
***
****
***
WT
swi1Δ
swi3Δ
rec12Δ
rec12Δ swi1Δ
rec12Δ swi3Δ
B
rec12Δ
rec12Δ swi1Δ
rec12Δ swi3Δ
Time (hrs.)
2C
4C
←DNA Content
C
I
II
III
DSBs
Time (hrs.):
D
% of total cells
1
2
3+
Time (hours)
1: ns
2: ***
3: *
1: ***
2: ns
3: ****

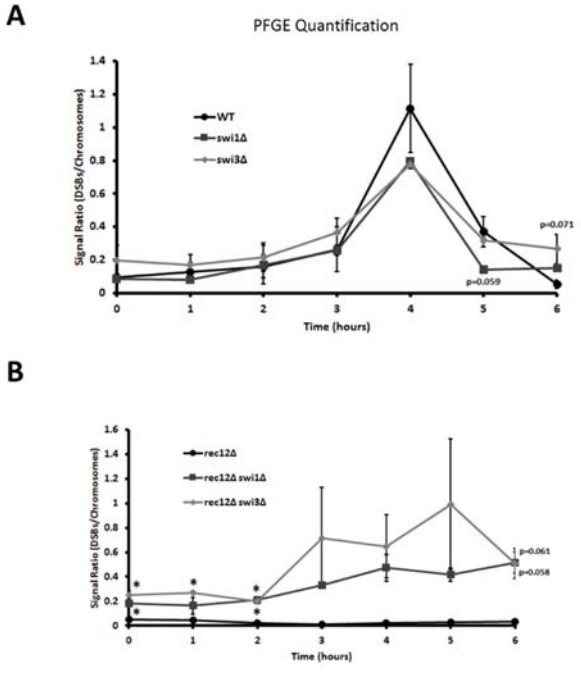
A
PFGE Quantification
Signal Ratio (DSBs/Chromosomes)
WT
swi1Δ
swi3Δ
p=0.071
p=0.059
Time (hours)
B
rec12Δ
rec12Δ swi1Δ
rec12Δ swi3Δ
p=0.061
p=0.058
Time (hours)

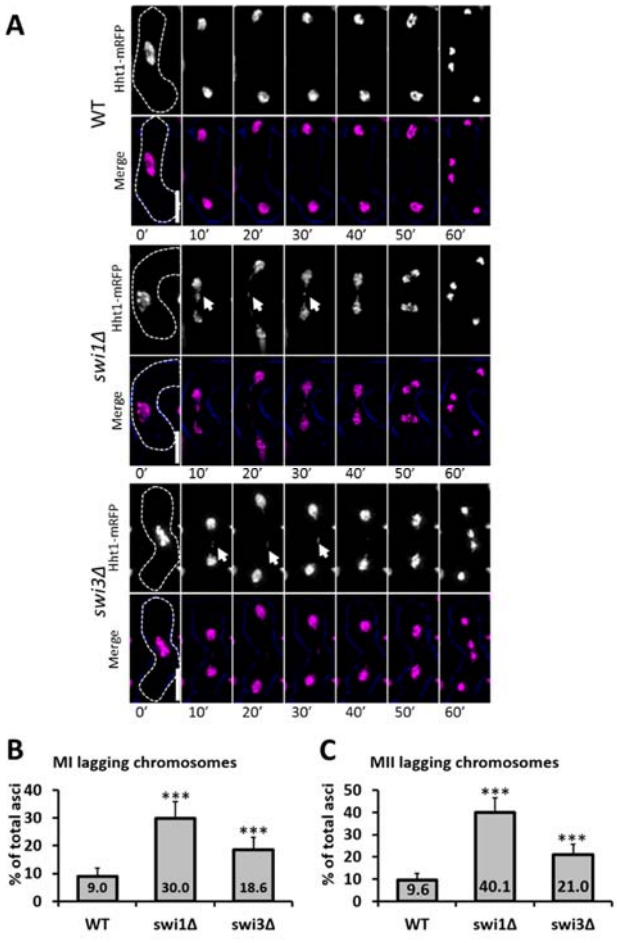
A
WT
swi1Δ
swi3Δ
Hht1-mRFP
Merge
0′
10′
20′
30′
40′
50′
60′
B
MI lagging chromosomes
% of total asci
9.0
30.0
18.6
WT
swi1Δ
swi3Δ
***
C
MII lagging chromosomes
% of total asci
9.6
40.1
21.0
WT
swi1Δ
swi3Δ
***

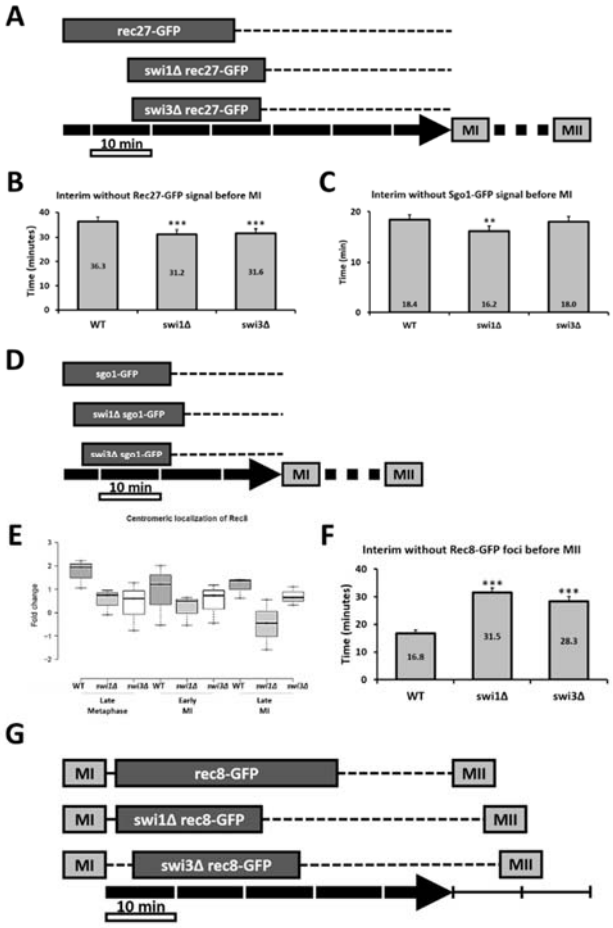
A
rec27-GFP
swi1Δ rec27-GFP
swi3Δ rec27-GFP
MI
MII
10 min
B
Interim without Rec27-GFP signal before MI
Time (minutes)
36.3
31.2
31.6
WT
swi1Δ
swi3Δ
C
Interim without Sgo1-GFP signal before MI
Time (min)
18.4
16.2
18.0
D
sgo1-GFP
swi1Δ sgo1-GFP
swi3Δ sgo1-GFP
E
Centromeric localization of Rec8
Fold change
Late Metaphase
Early MI
Late MI
F
Interim without Rec8-GFP foci before MII
16.8
31.5
28.3
G
rec8-GFP
swi1Δ rec8-GFP
swi3Δ rec8-GFP

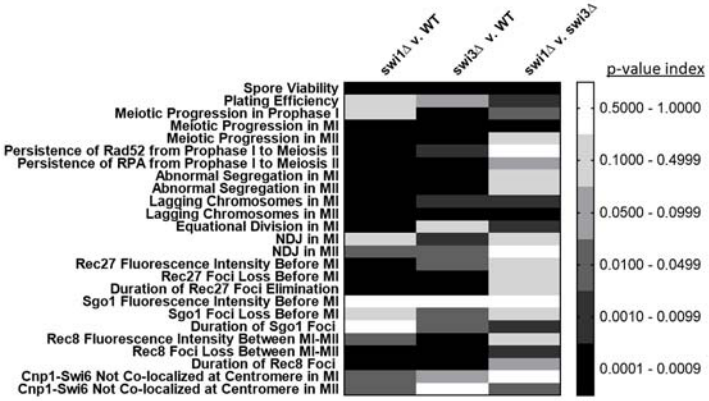
swi1Δ v. WT
swi3Δ v. WT
swi1Δ v. swi3Δ
p-value index
0.5000 - 1.0000
0.1000 - 0.4999
0.0500 - 0.0999
0.0100 - 0.0499
0.0010 - 0.0099
0.0001 - 0.0009
Spore Viability
Plating Efficiency
Meiotic Progression in Prophase I
Meiotic Progression in MI
Meiotic Progression in MII
Persistence of Rad52 from Prophase I to Meiosis II
Persistence of RPA from Prophase I to Meiosis II
Abnormal Segregation in MI
Abnormal Segregation in MII
Lagging Chromosomes in MI
Lagging Chromosomes in MII
Equational Division in MI
NDJ in MI
NDJ in MII
Rec27 Fluorescence Intensity Before MI
Rec27 Foci Loss Before MI
Duration of Rec27 Foci Elimination
Sgo1 Fluorescence Intensity Before MI
Sgo1 Foci Loss Before MI
Duration of Sgo1 Foci
Rec8 Fluorescence Intensity Between MI-MII
Rec8 Foci Loss Between MI-MII
Duration of Rec8 Foci
Cnp1-Swi6 Not Co-localized at Centromere in MI
Cnp1-Swi6 Not Co-localized at Centromere in MII